ANTIOXIDANTS & REDOX SIGNALING
Volume 00, Number 00, 2022

DOI: 10.1089/ars.2021.0059

mTOR-AKT Signaling in Cellular Clock Resetting Triggered by Osmotic Stress

Hikari Yoshitane,[1,2,*] Kiyomichi Imamura,[1,3,*] Takenori Okubo,[1,*] Yuta Otobe,[1,2] Satoshi Kawakami,[1,2] Shunsuke Ito,[1,2] Toru Takumi,[3] Kazuki Hattori,[4] Isao Naguro,[4] Hidenori Ichijo,[4] and Yoshitaka Fukada[1,2,5]

Abstract

Aims: The circadian clock oscillates in a cell-autonomous manner with a period of ~24 h, and the phase is regulated by various time cues such as light and temperature through multiple clock input pathways. We

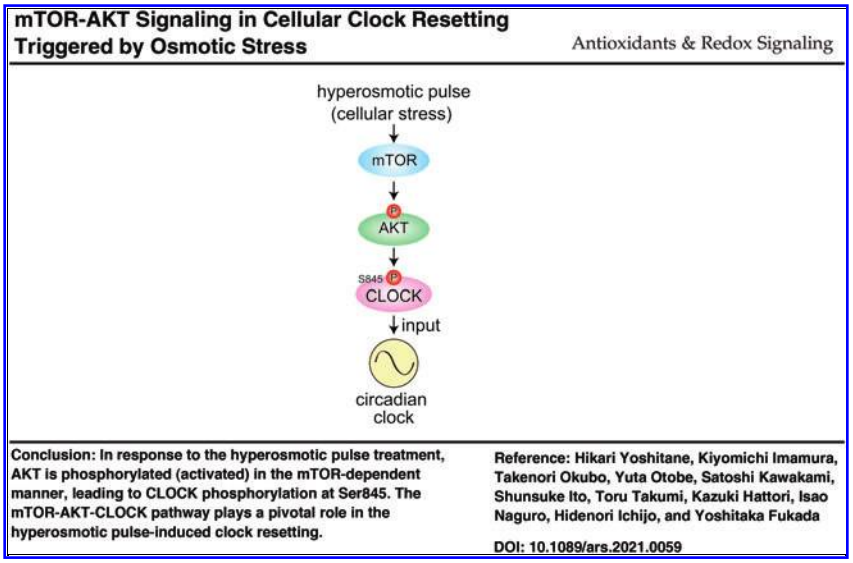

Color images are available online.

[1]Department of Biological Sciences, School of Science, The University of Tokyo, Bunkyo-ku, Japan.
[2]Circadiain Clock Project, Tokyo Metropolitan Institute of Medical Science, Setagaya-ku, Japan.
[3]Department of Physiology and Cell Biology, School of Medicine, Kobe University, Kobe, Japan.
[4]Laboratory of Cell Signaling, Graduate School of Pharmaceutical Sciences, The University of Tokyo, Bunkyo-ku, Japan.
[5]Laboratory of Animal Resources, Center for Disease Biology and Integrative Medicine, Graduate School of Medicine, The University of Tokyo, Tokyo, Japan.
*All these authors contributed equally to this work.

previously found that osmotic and oxidative stress strongly affected the circadian period and phase of cellular rhythms, and triple knockout of apoptosis signal-regulating kinase (ASK) family members, *Ask1*, *Ask2,* and *Ask3*, abolished the phase shift (clock resetting) induced by hyperosmotic pulse treatment. We aimed at exploring a key molecule(s) and signaling events in the clock input pathway dependent on ASK kinases.
Results: The phase shift of the cellular clock induced by the hyperosmotic pulse treatment was significantly reduced by combined deficiencies of the clock(-related) genes, *Dec1, Dec2*, and E4 promoter-binding protein 4 (also known as *Nfil3*) (*E4bp4*). In addition, liquid chromatography mass/mass spectrometry (LC-MS/MS)-based proteomic analysis identified hyperosmotic pulse-induced phosphorylation of circadian locomotor output cycles caput (CLOCK) Ser845 in an AKT-dependent manner. We found that AKT kinase was phosphorylated at Ser473 (*i.e.*, activated) in response to the hyperosmotic pulse experiments. Inhibition of mechanistic target of rapamycin (mTOR) kinase by Torin 1 treatment completely abolished the AKT activation, suppressed the phosphorylation of CLOCK Ser845, and blocked the clock resetting induced by the hyperosmotic pulse treatment.
Innovation and Conclusions: We conclude that mTOR-AKT signaling is indispensable for the CLOCK Ser845 phosphorylation, which correlates with the clock resetting induced by the hyperosmotic pulse treatment. Immediate early induction of the clock(-related) genes and CLOCK carboxyl-terminal (C-terminal) region containing Ser845 also play important roles in the clock input pathway through redox-sensitive ASK kinases. *Antioxid. Redox Signal.* 00, 000–000.

Keywords: circadian rhythm, apoptosis signal-regulating kinase (ASK), osmotic stress, AKT, mechanistic target of rapamycin (mTOR), LC-MS/MS

Introduction

THE CIRCADIAN RHYTHMS are generated by a cell-autonomous mechanism called the circadian clock. In mammals, a central pacemaker of the circadian clocks resides in the hypothalamic suprachiasmatic nuclei (SCN) of the brain, whereas peripheral clocks are distributed among almost all the tissues. The circadian clock oscillates even in cultured cells, a model of the peripheral clocks (1, 2, 22, 65). In individual cells, a heterodimer of circadian locomotor output cycles caput (CLOCK) and brain and muscle Arnt-like protein-1 (BMAL1) binds to a DNA-*cis*-element E-box, and activates transcription of a series of genes, including *Period* (*Per*) and *Cryptochrome* (*Cry*). Translated PER and CRY proteins inhibit the CLOCK-BMAL1–dependent transcriptional activation, leading to the formation of a transcriptional/translational negative feedback loop (4, 16).

The molecular clock oscillates with a period of $\sim$24 h and synchronizes to the environmental 24 h cycle by adjusting its phase in response to various time cues such as light and temperature. In multicellular organisms, the phases of the peripheral clocks synchronize with each other, at least within a tissue, so as to play time-of-the-day–dependent functions of the tissue. For the cellular clocks to adjust the phase to the environmental changes, post-translational modifications also play key roles by regulating stability, subcellular localization, and functions of the clock proteins in multiple clock input pathways (20, 32, 68, 69).

At the organismal level, the most fundamental time cue is a 24-h light–dark cycle that entrains the central clock in the SCN. On the contrary, the peripheral clocks can synchronize to nonphotic signals such as temperature cycles (5), humoral factors (57), heat shock (6), ultraviolet irradiation (46), and influx of ions (19). The circadian clock is also associated tightly with a cellular redox state. Relative levels of a cellular redox cofactor, nicotinamide adenine dinucleotide (NAD^+), regulate the circadian clock, and *vice versa*; the clock generates a circadian rhythm of cellular NAD^+ levels (40, 47, 50). Other redox-related metabolites and proteins such as peroxiredoxins show circadian rhythms (17, 44).

In our previous study, we demonstrated that an acute change in the redox state by pulse treatment with an oxidizing agent H_2O_2 induced phase shifts of the circadian rhythms in mouse embryonic fibroblasts (MEFs), while a sustained change in the redox state by chronic treatment with a catalase inhibitor, 3-amino-1,2,4-triazole (ATZ), lengthened the circadian period (25).

It is reported that several members of the mitogen-activated protein kinase kinase kinase (MAPKKK) family act as redox sensors, among which apoptosis signal-regulating kinase (ASK) kinases are activated by redox changes and also by osmotic stress (24, 26, 29, 37, 38, 43, 53, 60). We showed that ASK kinases play a crucial role in both the circadian period changes and phase shifts induced by osmotic or oxidative stress (25). The hyperosmotic pulse treatment led to atypical ASK signaling in a mitogen-activated protein kinase (MAPK)-independent manner.

Innovation

To date, various input signals regulating the circadian clock have been described. We previously identified apoptosis signal-regulating kinase (ASK) indispensable for cellular stress-dependent clock-resetting mechanism, which accompanied circadian locomotor output cycles caput (CLOCK) phosphorylation in the carboxyl-terminal (C-terminal) tail. However, a key molecule(s) and signaling events in the ASK-dependent clock input pathway were still missing. This study clarifies that mechanistic target of rapamycin (mTOR)-AKT signaling is responsible for CLOCK phosphorylation at Ser845 in the C-terminal tail, which correlates with the cellular clock resetting triggered by hyperosmotic pulse treatment. These results lead to deeper understanding of the clock-resetting mechanisms underpinned by the circadian clock input signals and cellular stress pathways.

Physiologically, the ASK-triple deficiencies in mice significantly reduced the period lengthening of the behavioral rhythm in constant light conditions and attenuated the phase shifts triggered by a light pulse given during nighttime (25). However, little is known about critical molecules and signaling events in the clock input pathway dependent on ASK kinases. Here, we found that hyperosmotic pulse treatment triggered mechanistic target of rapamycin (mTOR)-dependent phosphorylation (activation) of AKT kinases, stimulating phosphorylation of CLOCK protein at Ser845. The mTOR-AKT phosphorylation cascade plays a key role in the clock input pathway, which may occur through CLOCK phosphorylation and redox-sensitive ASK kinases.

Results

Dec1, Dec2, and E4bp4 genes partially contribute to circadian phase shift induced by hyperosmotic pulse treatment in an ASKs-dependent manner

We previously reported that ASK kinases are essential for the cellular clock resetting triggered by 30-min hyperosmotic pulse treatment of cultured MEFs with 600 m*M* sorbitol (25). Within 30 min after the sorbitol pulse, clock(-related) genes, *Dec1*, *Dec2,* and E4 promoter-binding protein 4 (also known as *Nfil3*) (*E4bp4*), were induced as immediate early genes, and the induction of their messenger RNA (mRNA) levels was blunted in the *Ask*1/*Ask*2/*Ask*3 triple knockout (*Ask*-TKO) MEFs (25). These results were consistently reproduced in this study (Supplementary Fig. S1A).

Dec1 mRNA level was also rapidly induced by a 30-min pulse treatment with 0.4 m*M* H_2O_2 (Supplementary Fig. S1B), which caused a remarkable phase shift of cellular rhythms (25). The oxidative stress-dependent induction of *Dec1* mRNA level was significantly attenuated in the *Ask*-TKO MEFs (Supplementary Fig. S1B). It was reported that light exposure during subjective night induced *Dec1* expression in the mouse SCN (23) and *E4bp4* expression in the chicken pineal gland (14).

Mice deficient for both *Dec1* and *Dec2* genes displayed a marked reduction in light-dependent phase shifts (52). Taking into consideration our previous findings that the photic response was compromised in *Ask*-TKO mice (25), we hypothesized that *Dec1*, *Dec2*, and *E4bp4* inductions may play an important role in the circadian input in response to not only the photic stimuli but also the hyperosmotic pulse.

To evaluate a potential contribution of these three genes to the cellular clock resetting triggered by the hyperosmotic pulse, we crossed TKO mice deficient for *Dec1*, *Dec2*, and *E4bp4* with PER2::LUC (luciferase) knock-in mice, in which luciferase was fused with endogenous PER2 protein to monitor bioluminescence rhythms. From the mutant mice, MEFs were prepared and termed *D1D2E4*-TKO/PER2::LUC MEFs in this study (Supplementary Fig. S1A, C). We monitored bioluminescence rhythms of the mutant MEFs, and then the cells were exposed to a 30-min pulse of a conditioned medium containing various concentrations of sorbitol, which was referred to as ''the hyperosmotic pulse (treatment)'' in this study (Fig. 1A).

The circadian phase of the bioluminescence rhythms in control PER2::LUC MEFs was shifted by 7.28 ± 0.63 h with 300 m*M* sorbitol pulse and by 10.62 ± 1.73 h with 600 m*M* sorbitol pulse (Fig. 1B, C). The hyperosmotic pulse-induced phase shifts were significantly attenuated in the *D1D2E4*-TKO MEFs (Fig. 1B, C). These observations indicate that the hyperosmotic pulse-dependent induction of these genes contributes to the circadian input pathway.

On the contrary, the hyperosmotic pulse-induced phase shift was almost completely abolished in the *Ask*-TKO MEFs (Fig. 1D, E), as was observed in our previous study (25). When compared with the critical phenotype in the *Ask*-TKO MEFs, the reduced but still remaining phase shifts observed in the *D1D2E4*-TKO MEFs (4.30 ± 0.46 h by 300 m*M* sorbitol; 4.57 ± 0.63 h by 600 m*M* sorbitol; Fig. 1C) imply the presence of ASK-dependent but *Dec1/Dec2/E4bp4*-independent clock input pathway.

Redox-sensitive ASK signaling is dispensable for circadian phase shifts induced by pH shock

It was reported that pH changes of the cultured media activate ASK1 kinase (59). Indeed, *Dec1* mRNA displays immediate early induction in response to not only the hyperosmotic (sorbitol) pulse treatment but also alkalization of the cultured media (from pH 7.0 to 7.4), both of which caused type-0 resetting of the cellular rhythms (25, 30). Similarly, *E4bp4* mRNA was rapidly induced by not only the hyperosmotic pulse treatment but also acid shock (from pH 7.0 to 6.6) that also causes type-0 resetting (30). *E4bp4* mRNA was also rapidly induced by H_2O_2 treatment, which causes cellular oxidative stress (61) and activates ASK1 kinase (60). These observations raised the possibility that the pH shock- or H_2O_2-dependent clock input signals share a common pathway with the hyperosmotic-dependent signaling through ASK kinases.

In control experiments, PER2::LUC MEFs were subjected to the acid or alkaline treatment (Supplementary Fig. S2A), which caused a phase delay of 2.15 ± 0.16 h with the acid shock (Supplementary Fig. S2B, E) or a delay of 2.47 ± 0.21 h with the alkaline shock (Supplementary Fig. S2F, I). The phase response by the acid shock was almost completely blunted in the *D1D2E4*-TKO MEFs (0.43 ± 0.24 h; Supplementary Fig. S2C, E), presumably due to the deficiency of the *E4bp4* gene as we reported previously (67). In contrast, no significant effect of the triple deficiencies of these genes (*D1D2E4*-TKO) was observed on the phase response by the alkaline shock (1.73 ± 0.26 h delay; Supplementary Fig. S2G, I), possibly due to genetic compensation or cell type-specific mechanisms.

Importantly, deficiencies of *Ask* genes had no obvious effect on the phase shift caused by the pH shock (2.68 ± 0.27 h delay by the acid shock or 2.42 ± 0.20 h delay by the alkaline shock; Supplementary Fig. S2D, E, H, I). In contrast, we previously reported that deficiencies of *Ask* genes significantly attenuated phase shifts in response to H_2O_2 pulses. Collectively, these results demonstrate that ASK kinases are dispensable for the pH shock-induced phase shifts and suggest a unique mechanism underlying the hyperosmotic pulse-induced redox-sensitive ASK signaling in the circadian clock resetting.

CLOCK carboxyl-terminal tail function in cellular clock and its phase shift

Our data indicated partial contribution of *Dec1/Dec2/E4bp4* genes to the hyperosmotic pulse-triggered clock resetting and revealed the presence of other clock input pathway(s) through ASK kinases. As one of critical molecular

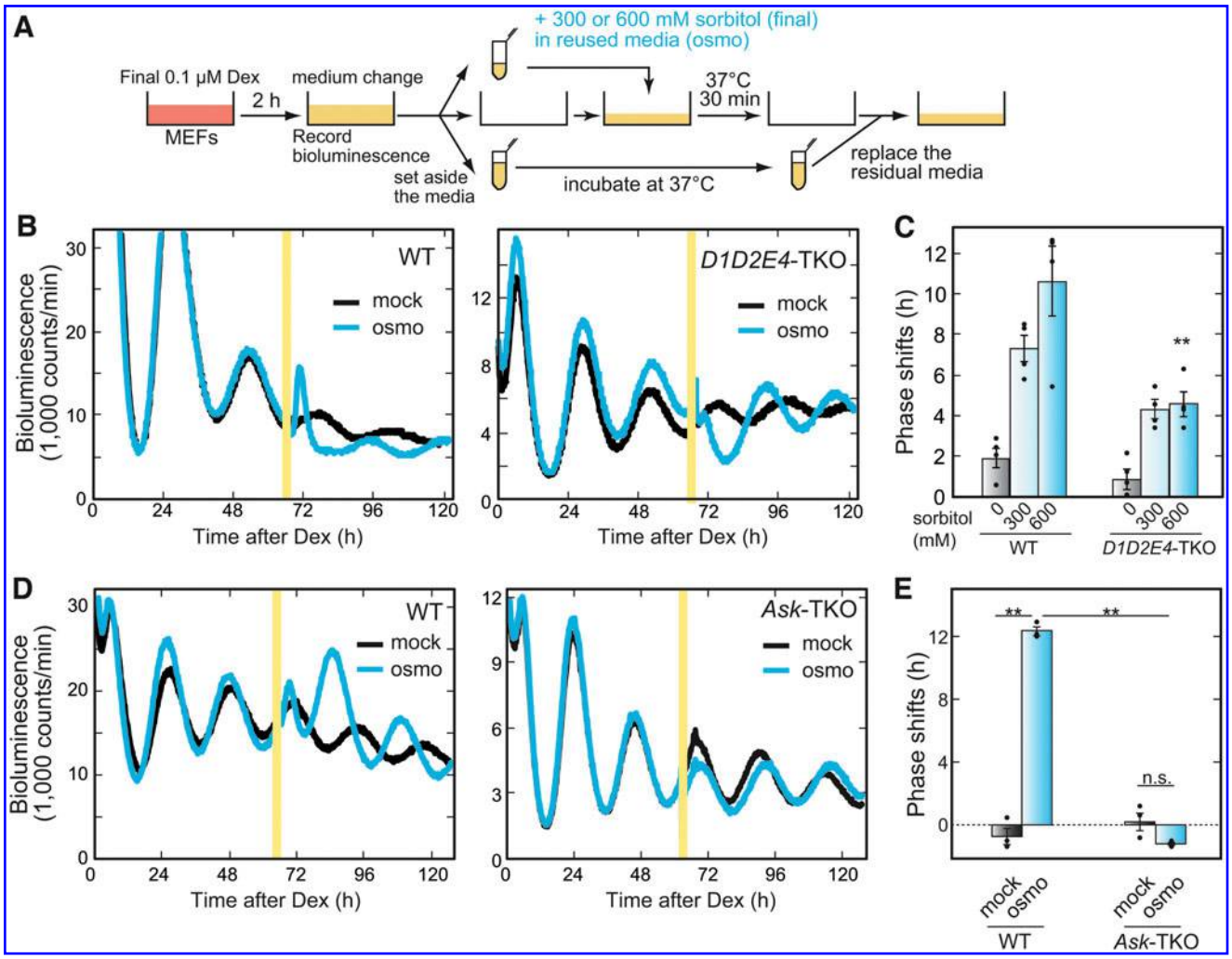

FIG. 1. ***Dec1***, ***Dec2,*** **and** ***E4bp4*** **genes contribute to the circadian phase shift induced by hyperosmotic pulse treatment.** **(A)** Experimental procedures for the hyperosmotic pulse treatment to investigate the phase shift of the cellular rhythms. **(B, D)** Representative cellular rhythms (*blue*) in response to the hyperosmotic pulse treatment (*yellow zone*) in the control PER2::LUC (WT) MEF **(B, D)**, the *Dec1*-KO/*Dec2*-KO/*E4bp4*-KO/PER2::LUC (*D1D2E4*-TKO) MEF **(B)**, and the *Ask1*-KO/*Ask2*-KO/*Ask3*-KO/PER2::LUC (*Ask*-TKO) MEF **(D)**. The timing of the 30-min pulse treatment of the 600 m*M* sorbitol is indicated as *yellow zone*. For mock treatment, the same volume of the recording medium was added (*black*). **(C)** The quantification data of the phase shifts induced by indicated concentrations of sorbitol. Phase-advance and phase-delay shifts are expressed in positive and negative values, respectively. Data are means with SEM, $^{**}p < 0.01$ *versus* WT ($n = 4$; Tukey–Kramer test). **(E)** The quantification data of the phase shifts induced by the hyperosmotic pulse. Phase-advance and phase-delay shifts are expressed in positive and negative values, respectively. Data are means with SEM, $^{**}p < 0.01$, n.s. $p \geq 0.05$ ($n = 3$; Tukey–Kramer test). Dec, deleted in esophageal cancer; *E4bp4*, E4 promoter-binding protein 4 (also known as NFIL 3); LUC, luciferase; MEF, mouse embryonic fibroblast; SEM, standard error of the mean; TKO, triple knockout; WT, wild type. Color images are available online.

candidates in the pathway, our previous phosphoproteomic analysis identified a singly phosphorylated peptide derived from the extreme carboxyl-terminal (C-terminal) region (termed C-tail: amino acid residues 841-855) of mouse CLOCK protein (25).

Importantly, the abundance of the C-tail phosphopeptide was significantly upregulated by the hyperosmotic pulse treatment, and this upregulation was abolished in the *Ask*-TKO MEFs (25), suggesting that phosphorylation of CLOCK C-tail is involved in a mechanism underlying the hyperosmotic pulse-dependent phase shift. To further investigate the role of CLOCK C-tail in the circadian resetting, we used CRISPR-Cas9 systems to isolate CLOCKΔC-tail/PER2::LUC MEFs, in which a part of *Clock* gene was excised to generate C-tail (841–855)-specific deletion of CLOCK (Fig. 2A and Supplementary Fig. S3). In the CLOCKΔC-tail mutant MEFs, we observed dampened cellular rhythms (Fig. 2B, E) with shorter circadian periods (Fig. 2B, D).

Interestingly, similar phenotypes were observed in the *Ask*-TKO MEFs [Fig. 2C–E and see also Imamura *et al.* (25)], raising the possibility that the C-tail function of CLOCK protein is associated with the ASK kinase signaling. Indeed, in the CLOCK ΔC-tail mutant MEFs, we observed a significant decrease in the phase-shifting effects caused by the hyperosmotic pulse treatment (control: 12.40 ± 0.31 h

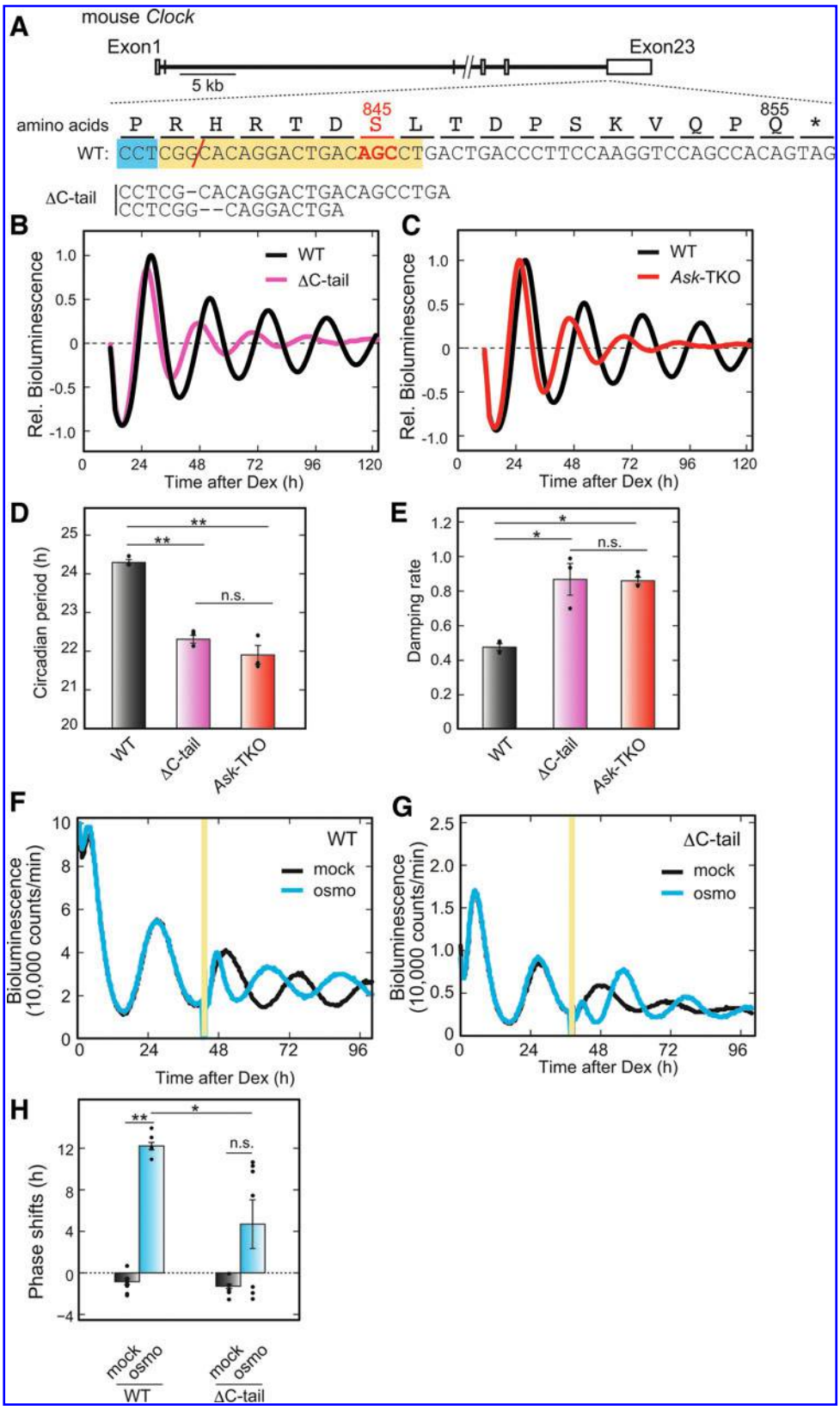

FIG. 2. C-terminal tail of CLOCK protein containing Ser845 regulates cellular rhythm. (A) Isolation of the CLOCKΔC-tail/PER2::LUC MEF lacking the CLOCK C-terminal 15 amino acids (CLOCK 841–855). The DNA sequence of mouse genome around exon 23 of *Clock* gene and its encoded amino acid residues are shown. Ser845 of CLOCK protein and the corresponding DNA sequences are shown in *red characters*. The *yellow-highlighted* sequence corresponds to the designed targeting sequence of the sgRNA, and the *blue-highlighted* sequence shows PAM. The *red line* in the sequence shows an estimated site of the double-strand DNA break. A frameshift deletion was occurred in CLOCKΔC-tail. **(B, C)** Representative cellular rhythms in the control PER2::LUC (WT) MEF (*black*), the CLOCKΔC-tail/PER2::LUC MEF (*magenta*), and the *Ask1*-KO/*Ask2*-KO/*Ask3*-KO/PER2::LUC (*Ask*-TKO) MEF (*red*). **(D, E)** The quantification data of the circadian period and damping rate of the cellular rhythms in **(B, C)**. Data are means with SEM, $*p<0.05$, $**p<0.01$, n.s. $p\geq0.05$ ($n=3$; Tukey–Kramer test). **(F, G)** Representative cellular rhythms (*blue*) in response to the hyperosmotic pulse treatment (*yellow zone*) in the control PER2::LUC (WT) MEF and the CLOCKΔC-tail/PER2::LUC MEF. For mock treatment, the same volume of the recording medium was added (*black*). **(H)** The quantification data of the phase shifts of the cellular rhythms in **(F, G)**. Phase-advance and phase-delay shifts are expressed in positive and negative values, respectively. Data are means with SEM; $*p<0.05$, $**p<0.01$, n.s. $p\geq0.05$ ($n=6$–8; Tukey–Kramer test). C-terminal, carboxyl-terminal; CLOCK, circadian locomotor output cycles caput; PAM, protospacer adjacent motif; sgRNA, single guide RNA. Color images are available online.

advance, ΔC-tail: 4.75 ± 2.35 h advance; Fig. 2F–H). These results shed light on the critical role of CLOCK C-tail in the ASK-mediated phase regulation of the cellular clock.

AKT mediates hyperosmotic pulse-induced phosphorylation of CLOCK Ser845

Previously, our liquid chromatography mass/mass spectrometry (LC-MS/MS) analysis revealed the hyperosmotic pulse-induced phosphorylation of CLOCK C-tail, but the precise phosphorylated residue was undetermined, leaving the candidates, Thr843 and Ser845 (25). In the present study, Myc-CLOCK and Flag-BMAL1 were overexpressed in HEK293T cells, and the functional CLOCK-BMAL1 heterodimer was purified by Flag immunoprecipitation from the cell lysate prepared 30 min after the 30-min hyperosmotic pulse treatment. Subsequent LC-MS/MS analysis identified Ser845 as the phosphorylation site in CLOCK C-tail (Supplementary Fig. S4). The newly developed experimental condition enables us to quantify the level of Ser845 phosphorylation in CLOCK C-tail.

The amino acid sequence of CLOCK around Ser845, RHRTDpS, matched a phosphorylation consensus motif of AKT kinases, ''RXRXXpS/T'' (18, 35, 42) (Fig. 3A). AKT, also known as protein kinase B (PKB), plays a key role in multiple cellular processes such as metabolism, cell proliferation, apoptosis, transcription, and cell migration (18, 42). It should be emphasized that AKT is a component of the high molecular mass complex formed with ASK1 (60). These facts gave rise to the idea that the hyperosmotic pulse-induced phosphorylation of CLOCK Ser845 is regulated by AKT activity.

To explore this possibility, we used MK2206, an allosteric inhibitor that inhibits AKT activity by preventing its translocation to cellular membranes (34, 45). Transfected HEK293T cells overexpressing Myc-CLOCK and Flag-BMAL1 were exposed to 1.0 μM MK2206 for 16 h before the hyperosmotic pulse treatment, and we evaluated the Ser845-phosphorylation level in the Flag-purified CLOCK–BMAL1 complex by LC-MS/MS analysis. The amount of pSer845-containing CLOCK C-tail peptide at 30 min after the 30-min pulse treatment of 600 mM sorbitol (Fig. 3B; ''A'') was significantly reduced in the presence of MK2206 (Fig. 3C). In the LC-MS/MS analysis, no significant change was observed in amounts of CLOCK protein nor other phosphopeptides derived from CLOCK and BMAL1 proteins (Supplementary Fig. S5).

These data demonstrate that AKT kinases are responsible for the hyperosmotic pulse-induced phosphorylation of CLOCK protein at Ser845.

AKT is a crucial player in the hyperosmotic pulse-induced clock resetting

We explored hyperosmotic pulse-induced changes of AKT kinase activity by immunoblotting for Ser473-phosphorylated form (an activated form) of AKT (18, 42). HEK293T cells were exposed to the 30-min hyperosmotic pulse of 600 mM sorbitol, and the phosphorylation levels of AKT at Ser473 were evaluated at three time points (Fig. 3B); before the sorbitol pulse (B, before the pulse), before the end of the 30-min sorbitol pulse treatment (D, during the pulse), and 30 min after the sorbitol pulse (A, after the pulse). The phosphorylation of AKT-Ser473 observed before the pulse treatment was almost abolished during the pulse and remarkably stimulated after the pulse (Fig. 3D lanes 1–3, Supplementary Fig. S6A).

The treatment of the cells with 1.0 μM MK2206 completely blocked AKT-Ser473 phosphorylation (Fig. 3D lanes 4–6). During the experiment, no significant change was observed in the total protein amounts of AKT (Fig. 3D and Supplementary Fig. S6A). Similar results with AKT-Ser473 phosphorylation levels were obtained when wild-type (WT) MEFs were subjected to hyperosmotic pulse treatment (Supplementary Fig. S6B lanes 1–3). These observations demonstrate that AKT activity in both human and mouse cells is responsive to the hyperosmotic pulse treatment.

To unbiasedly evaluate activity changes of various kinases (including AKT) in response to the hyperosmotic pulse treatment, we performed phosphoproteome analysis and Kinase-Substrate Enrichment Analysis (KSEA) (10). In the KSEA, AKT1 activity in the MEFs was estimated based on the phosphorylation levels of a series of AKT1 substrate peptides. We observed that AKT1 activity was downregulated during the hyperosmotic pulse treatment and upregulated after the

FIG. 3. AKT is a protein kinase responsible for CLOCK Ser845 phosphorylation and the hyperosmotic pulse-induced clock resetting. **(A)** Comparison of amino acid sequences in C-terminal regions of mouse CLOCK and human CLOCK with the AKT consensus motif. Identical amino acid residues between the two species are highlighted by *gray backgrounds*. **(B)** Time course of the hyperosmotic pulse treatment in this study. The timings before, during, and after the hyperosmotic pulse treatment are shown as ''B,'' ''D,'' and ''A,'' respectively. **(C)** The effect of AKT inhibitor on phosphorylation levels of CLOCK protein at Ser845. HEK293T cells were transiently transfected with plasmids for expressing CLOCK and BMAL1. The cells were treated by the hyperosmotic pulse and subsequently collected as shown in **(B)**. MK2206 (1.0 μM) was added 16 h before the hyperosmotic pulse treatment. For the control, the same volume of DMSO was added. Purified CLOCK–BMAL1 complex was subjected to LC-MS/MS-based proteomic analysis. Data are means with SEM, $^{**}p < 0.01$ ($n = 1$ for ''D'' and $n = 3$ for ''A,'' Student's t-test). **(D)** Immunoblot analysis for the temporal changes of phosphorylation and total protein levels of endogenous AKT in HEK293T cells. The cells were treated by the hyperosmotic pulse and subsequently collected as shown in **(B)**. MK2206 (1.0 μM) was added 16 h before the hyperosmotic pulse treatment. For control, the same volume of DMSO was added. **(E)** The effect of MK2206 on the circadian phase shift in response to the hyperosmotic pulse treatment. Shown are representative cellular rhythms (*blue*) in response to the hyperosmotic pulse treatment (*yellow zone*) in the PER2::LUC MEF with DMSO (*upper*) and 1.0 μM MK2206 (*lower*). For mock treatment, the same volume of recording medium was added (*black*). **(F)** The quantification data of the circadian phase shifts in response to the hyperosmotic pulse treatment with and without MK2206. Phase-advance and phase-delay shifts are expressed in positive and negative values, respectively. Data are means with SEM, $^{**}p < 0.01$, n.s. $p \geq 0.05$ ($n = 6$–7; Tukey–Kramer test). BMAL1, brain and muscle Arnt-like protein-1; DMSO, dimethyl sulfoxide; HEK, human embryonic kidney; LC-MS/MS, liquid chromatography mass/mass spectrometry. Color images are available online.

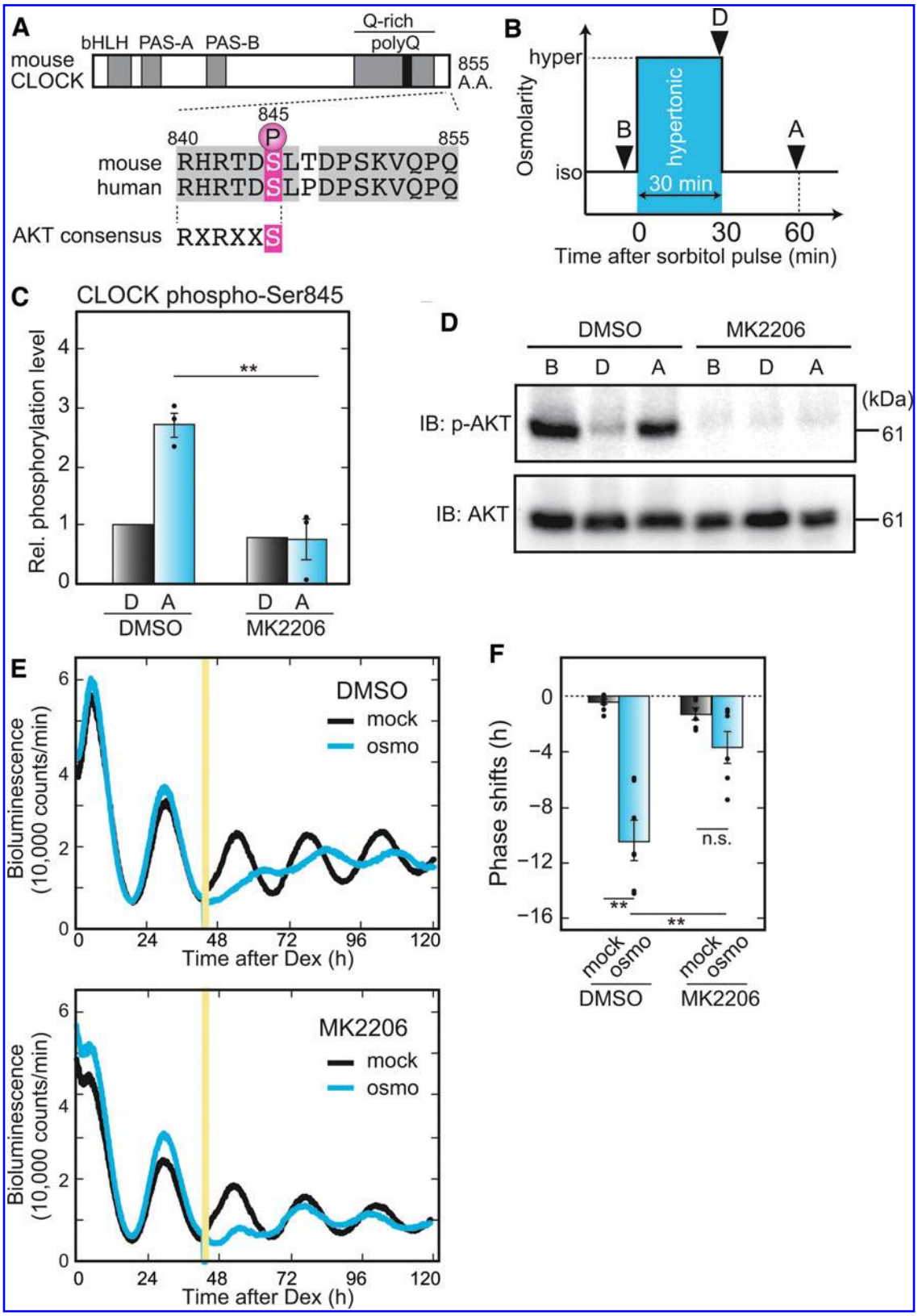

pulse (Supplementary Fig. S7), being consistent with our immunoblot analysis of the activated form of AKT-Ser473 (Fig. 3D and Supplementary Fig. S6A, B).

We then explored the importance of AKT activity in the hyperosmotic pulse-induced phase shift of the circadian clock. In PER2::LUC MEFs, the phase shift induced by the sorbitol pulse treatment was largely attenuated by the chronic treatment with 1.0 μM MK2206 (control: 10.46 ± 1.41 h delay, MK2206: 3.64 ± 1.14 h delay; Fig. 3E, F). Therefore, we identified AKT as a key player in the clock input pathway leading to the phosphorylation of CLOCK Ser845 in response to the hyperosmotic pulse treatment. The decrease of the osmolarity might have activated (phosphorylated) AKT, but the possibility is not eliminated that a combination of the increase and decrease of the osmolarity (*i.e.*, the hyperosmotic ''pulse'') had a combined effect on both the AKT activity change and the clock resetting.

mTOR-AKT pathway for circadian phase regulation in response to hyperosmotic stress

To further understand the molecular mechanism underlying the cellular clock resetting triggered by the hyperosmotic pulse, we focused on the mTOR, a Ser/Thr kinase that forms at least two distinguishable multiprotein complexes, mTORC1 and mTORC2 (Fig. 4A) (54). Interestingly, phosphorylation of AKT-Ser473 is a target of mTORC2 (27, 55), and it is reported that mTOR activity in cultured cells is downregulated by a rapid increase in osmolarity of the medium (48). mTOR may thus play an essential role in AKT-Ser473 phosphorylation in response to the hyperosmotic pulse, leading to CLOCK-Ser845 phosphorylation.

Indeed, AKT-Ser473 phosphorylation after the hyperosmotic pulse was completely blocked by treatment of HEK293T cells with 0.5 μM Torin 1, an inhibitor of mTORC1 and mTORC2 (Fig. 4A, B). The hyperosmotic pulse-induced phosphorylation of CLOCK Ser845 was significantly reduced by the Torin 1 treatment (Fig. 4C). Furthermore, treatment of PER2::LUC MEFs with 0.5 μM Torin 1 almost completely blocked the clock resetting triggered by the hyperosmotic pulse, whereas treatment with 1.0 μM rapamycin, an inhibitor specific for FKBP12-mediated activation of mTORC1, had no detectable effect (control: 12.24 ± 0.40 h delay, Torin 1: 1.85 ± 0.14 h delay, rapamycin: 14.33 ± 0.31 h delay; Fig. 4D–G). It was concluded that mTOR (probably in mTORC2) is a critical signaling molecule indispensable for the hyperosmotic pulse-induced clock resetting.

Collectively, we identified mTOR kinase as a new signaling member for regulating circadian phase of the cellular clock in response to the hyperosmotic pulse. The hyperosmotic pulse treatment induced mTOR-dependent phosphorylation of AKT kinases, leading to downstream changes in phosphorylation of multiple substrates, including CLOCK protein at Ser845 (Fig. 5). The mTOR-AKT-CLOCK phosphorylation cascade and immediate early induction of the clock(-related) genes should play important roles in the clock input pathway through redox-sensitive ASK kinases.

Discussion

We previously reported that the period and phase of the mammalian circadian clock were regulated by cellular stress such as oxidative and osmotic (hypertonic and hypotonic) stimuli (25). The hyperosmotic pulse treatment induced a phase-dependent phase shift, which was entirely abolished by triple deficiencies of ASK family members (*Ask1*, *Ask2*, and *Ask3*) (Fig. 1D, E). Interestingly, the hyperosmotic pulse led to atypical ASK signaling in a MAPK-independent manner (25).

In the present study we demonstrated that the clock (-related) genes, *Dec1*, *Dec2*, and *E4bp4*, contributed partially to the hyperosmotic pulse-induced resetting of the cellular clock (Fig. 1). Both AKT kinase activity and CLOCK-Ser845 phosphorylation responded to the hyperosmotic pulse treatment, and the CLOCK phosphorylation was blocked by inhibiting AKT kinase activity, together indicating that AKT is responsible for the hyperosmotic pulse-induced phosphorylation of CLOCK-Ser845 (Fig. 3).

We further demonstrated that mTOR kinase activity was essential to regulate both AKT activity and CLOCK-Ser845 phosphorylation in response to the hyperosmotic

FIG. 4. mTOR is indispensable for AKT-mediated CLOCK phosphorylation and the hyperosmotic pulse-induced clock resetting. **(A)** mTOR forms at least two multiprotein complexes, mTORC1 and mTORC2, which are distinguished by their partner proteins, substrate specificities, and sensitivity to inhibitors. **(B)** Immunoblot analysis for the temporal changes of phosphorylation and total protein levels of endogenous AKT in HEK293T cells. The cells were treated by the hyperosmotic pulse and subsequently collected as shown in Figure 3B. Torin 1 (0.5 μM) was added 16 h before the hyperosmotic pulse treatment. For control, the same volume of DMSO was added. Total protein amounts of the samples were adjusted to a comparative level. For the determination of the relative phosphorylation levels of AKT, the signals of p-AKT were normalized by the signals of total-AKT. Data are means with SEM, $*p < 0.05$ ($n = 3$; Tukey–Kramer test). **(C)** The effect of mTOR inhibitor on phosphorylation levels of CLOCK protein at Ser845. HEK293T cells were transiently transfected with plasmids for expressing CLOCK and BMAL1. The cells were treated by the hyperosmotic pulse and subsequently collected at the timing A (after the treatment) as shown in Figure 3B. For mock treatment, the same volume of the recording medium was added (*black*). Torin 1 (0.5 μM) was added 16 h before the hyperosmotic pulse treatment. For the control, the same volume of DMSO was added. Purified CLOCK–BMAL1 complex was subjected to LC-MS/MS-based proteomic analysis. Data are means with SEM, $*p < 0.01$ ($n = 3$; Tukey–Kramer test). **(D–F)** The effects of mTOR inhibitors on the circadian phase shifts in response to the hyperosmotic pulse treatment. Shown are representative cellular rhythms (*blue*) in response to the hyperosmotic pulse treatment (*yellow zone*) in the PER2::LUC MEF with DMSO **(D)**, 0.5 μM Torin 1 **(E)**, and 1.0 μM rapamycin **(F)**. For mock treatment, the same volume of the recording medium was added (*black*). **(G)** The quantification data of the circadian phase shifts in response to the hyperosmotic pulse treatment with and without mTOR inhibitors. Phase-advance and phase-delay shifts are expressed in positive and negative values, respectively. Data are means with SEM, $**p < 0.01$, n.s. $p \geq 0.05$ ($n = 7$-12; Tukey–Kramer test). mTOR, mechanistic target of rapamycin; N.D., not detected. Color images are available online.

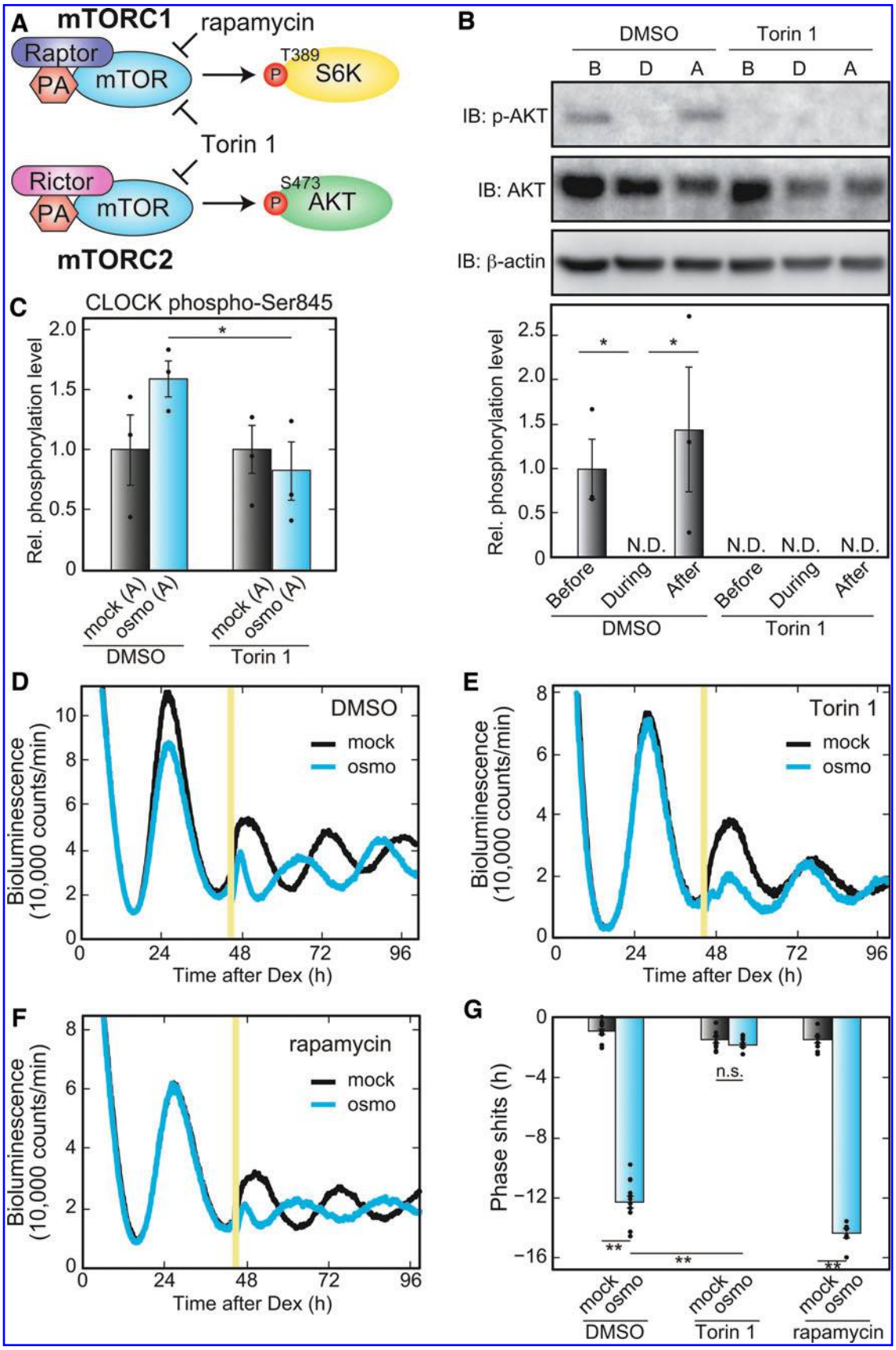

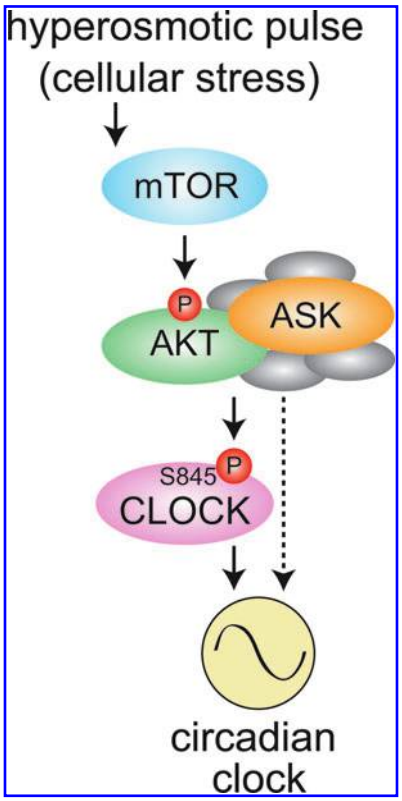

FIG. 5. mTOR-AKT-CLOCK pathway for clock resetting triggered by cellular stress. In response to the hyperosmotic pulse treatment, AKT-Ser473 is phosphorylated (activated) in the mTOR-dependent manner, leading to CLOCK phosphorylation at Ser845. The hyperosmotic pulse-induced phosphorylation of CLOCK-Ser845 is abolished in the *Ask*-TKO cells and is abrogated by inhibition of AKT or mTOR. The mTOR-AKT-CLOCK pathway plays a pivotal role in the hyperosmotic pulse-induced clock resetting through ASK kinases. Additional pathway(s) downstream of AKT kinases (shown by a *broken line*) may also contribute to the clock resetting. ASK, apoptosis signal-regulating kinase. Color images are available online.

pulse treatment (Fig. 4). Altogether, our data show that mTOR-AKT signaling pathway is important for coupling of the hyperosmotic pulse to the molecular clock mechanism, which correlates with changes in CLOCK protein phosphorylation in an ASK-dependent manner. Previous studies showed that light-dependent activation of mTOR signaling in the mouse SCN triggered phase shifts of the behavioral rhythm (8, 9).

In the peripheral tissues and cultured cells, on the contrary, mTOR signaling was activated in response to insulin (food intake) (12). These lines of evidence strongly support the notion that mTOR kinase is a key molecule for regulating the phase of the circadian clock not only in cultured cells but also *in vivo*. mTOR signaling was reported to play an important role in the period determination of the circadian clock in fruit fly (70) and mouse (49), implying a more fundamental role of mTOR signaling in the circadian clockwork.

Treatment of MEFs with Torin 1, an mTORC1/mTORC2 inhibitor, completely blocked the clock resetting induced by the hyperosmotic pulse treatment (Fig. 4). On the contrary, the clock resetting was significantly attenuated but not completely blocked by treatment with MK2206, an AKT inhibitor (Fig. 3) or by deletion of the CLOCK C-tail containing Ser845 (Fig. 2), suggesting that an additional pathway(s) downstream of mTOR kinase may contribute to the clock resetting.

Indeed, in addition to CLOCK-Ser845 phosphorylation, AKT-catalyzed phosphorylation of BMAL1 (at Ser42) is a promising candidate for the regulation of clock resetting. It was reported that insulin treatment of cultured cells promotes AKT-mediated phosphorylation of BMAL1 at Ser42, resulting in suppression of CLOCK-BMAL1-mediated transcriptional activity (13). Another role of BMAL1 phosphorylation at Ser42 could be a stimulation of mTOR-dependent translation (33).

AKT kinases also regulate several protein kinases such as glycogen synthase kinase 3 (GSK3) (18, 42), which phosphorylates several clock proteins such as CRY2 at Ser553 (21). It is known that AKT phosphorylates GSK3 at Ser9 and inhibits it (58). In fact, our KSEA revealed that GSK3 beta (GSK3B) activity was downregulated after the hyperosmotic pulse treatment (Supplementary Fig. S7). These protein kinases downstream of AKT may further contribute to the hyperosmotic pulse-induced clock resetting. Considering the downstream functions of mTOR kinase, we should note that mTOR is associated with a series of cellular functions such as translation and autophagy (54).

The mTOR-dependent translation is regulated by the circadian clock, and consequently *de novo* protein synthesis shows a circadian rhythm (33). Autophagy function was also reported to exhibit a robust circadian rhythm (36). Activation of signaling pathways downstream of mTOR kinase involved in these cellular functions may partly contribute to the hyperosmotic pulse-induced clock resetting. Consistently, our KSEA indicated that the activities of mTOR kinase and its substrate kinases (such as S6K and SGK1) were mostly sensitive to the hyperosmotic pulse treatment (Supplementary Fig. S7).

From another perspective, we consider the potential contribution of a regulatory volume increase (RVI) mechanism to clock resetting. A major consequence of acute hypertonic stress is cell shrinkage due to loss of cellular water, followed by RVI, which is dependent on the activity of ASK family members (63). In the RVI mechanism, WNK1-SPAK/OSR1 pathway is activated through the inactivation of ASK3 in response to osmotic stress (38), and this cellular signal may be transmitted to the clock components for triggering the phase shifts.

In this study, we showed that the hyperosmotic pulse-induced phosphorylation of AKT at Ser473 led to changes in phosphorylation of CLOCK-Ser845 (Fig. 3). Surprisingly, the hyperosmotic pulse-induced phosphorylation of AKT-Ser473 was observed even in the *Ask*-TKO cells (Supplementary Fig. S6B), in which the CLOCK-Ser845 phosphorylation was inhibited, and the clock resetting was completely abolished [Fig. 1C and see also Imamura *et al*. (25)]. These observations raised the possibility that ASK plays a role as a clutch for transmitting the magnitude of mTOR-AKT signaling to changes in CLOCK protein phosphorylation (Supplementary Fig. S6C).

Interestingly, AKT is a component of the high molecular mass complex of ASK1, and its components are dynamically changed by various types of cellular stress (60). Recently, it

was shown that ASK3 forms membrane-less condensates by liquid–liquid phase separation in response to hyperosmotic stimuli (62). These changes in the complex formation and/or the condensate phase may be a molecular basis for the clutch function of ASK in the mTOR-AKT–induced phase regulation (Supplementary Fig. S6C). As another explanation, the insensitivity of the *Ask*-deficient cellular clock to the hyperosmotic pulse may be attributable to a combined action of the many transcriptional and proteomic adaptations that allow the *Ask*-TKO cells to remain viable even in the absence of these key protein kinases.

It was previously shown that CLOCK-Ser845 is the phosphorylation site catalyzed by AKT, and that knock-in mice with a CLOCK Ser-to-Ala mutation (Ser845Ala) displayed normal free-running rhythms of locomotor activities (35). *Ask*-TKO mice also showed normal behavioral rhythms under constant dark conditions (25). Importantly, ASK-triple deficiencies in mice reduced light pulse-dependent phase shifts during the subjective night and attenuated a period-lengthening effect during constant light exposure (25). Future research is warranted, which will explore phenotypes of the CLOCK Ser845Ala mutant mice when they are exposed to light stimuli or various environmental conditions affecting circadian rhythms.

Disruption of the circadian clock by shift work, jet lag, or clock gene mutations increases the risk of a series of diseases such as insomnia, hypertension, and cancer, resulting in shortened life span (3, 7, 15, 31). The development of drugs that are capable of adjusting our circadian clock is eagerly awaited. This study demonstrates that in response to the hyperosmotic pulse treatment, mTOR-AKT phosphorylation cascade through ASK kinases can input to the clock oscillator *via* CLOCK protein phosphorylation. In the future, the cellular stress signaling pathways facilitating clock adjustment should be considered as potential targets for the discovery of chronoregulatory drugs.

Materials and Methods

Animals and cultured cells

D1D2E4-TKO mice were generated by crossing *Dec1*-KO (41), *Dec2*-KO (56), and *E4bp4*-KO (28, 67). The *D1D2E4*-TKO mice were further crossed with PER2::LUC knock-in mice (66), and MEF lines were isolated as described previously (25). MEFs were prepared from E12 to E15 embryos. After the head, paws, tail, and internal organs were removed; embryos were chopped and incubated in 0.25% trypsin in phosphate buffered saline (PBS) for 16 h at 4°C. After incubation for 30 min at 37°C in the trypsin solution, cells were dissociated by pipetting. As control, MEFs were isolated from PER2::LUC knock-in mice. These MEF lines were spontaneously immortalized by passages.

The following primers were used for genotyping of *D1D2E4*-TKO MEFs: for *Dec1* WT forward, 5′-AGCCC ACCCT GCAGA CCCAC-3′; for *Dec1* KO forward, 5′-ACGGA GCCGG TTGGC GCTAC-3′; for *Dec1* common reverse, 5′-AGCTG GCTGT GAGCT GTGCT C-3′; for *Dec2* WT forward, 5′-TCCCG AGGAG TCGCC GGGTT TC-3′; for *Dec2* KO forward, 5′-AGCTG CTATT GGCCG CTGCC C-3′; for *Dec2* common reverse, 5′-AGGCT TGGGT CGAGC CCTGG-3′; for *E4bp4* WT forward, 5′-GCCTT ACCGC ACAAG CTTCG-3′; for *E4bp4* KO forward, 5′-TAGCC GGATC AAGCG TATGC-3′; for *E4bp4* common reverse, 5′-ACACC CAGAC AGACG CCGTT-3′. The lengths of DNA fragments after polymerase chain reaction (PCR) are shown in Supplementary Figure S1C.

Cell culture and real-time monitoring of cellular rhythms

The MEFs and HEK293T/17 cells were cultured and passaged under 5% CO_2 in Dulbecco's modified Eagle's medium (D5796; Sigma) containing 100 U/mL penicillin, 100 mg/mL streptomycin, and 10% fetal bovine serum. Cellular bioluminescence rhythms were monitored as described previously (25) with minor modifications. In brief, the PER2::LUC MEFs were plated on 35 mm dishes (1.0×10^6 cells/dish) or 24-well plates (2.5×10^5 cells/well), and cultured at 37°C under 5% CO_2.

After 24 h, the cells were treated with 0.1 μM (final) dexamethasone for 2 h, and then the media were replaced by recording media (phenol-red free Dulbecco's modified Eagle's medium [Sigma] supplemented with 10% fetal bovine serum, 3.5 g/L glucose, 25 U/mL penicillin, 25 μg/mL streptomycin, 0.1 mM luciferin, and 10 mM HEPES-NaOH; pH 7.0). For the inhibition of kinases, MK2206, Torin 1, or rapamycin were added to the recording media. The bioluminescence signals of the cultured cells were continuously recorded for 5–10 days at 37°C in air with Dish Type Luminescencer, Kronos (AB-2500 or AB-2550; Atto), LumiCycle (Actimetrics), or LumiCEC (CL24A ver.2; Churitsu).

Reverse transcription quantitative PCR (RT-qPCR)

Total RNA was prepared from the MEFs using TRIzol reagent (Invitrogen) and the RNeasy Mini Kit (Qiagen) according to the manufacturers' protocol. Total RNA was reverse-transcribed using SuperScript II Reverse Transcriptase (Invitrogen) with random oligo primer, and the reaction mixture was treated with RNaseOUT (Invitrogen). The complementary DNA (cDNA) was subjected to real-time RT-qPCR (StepOnePlus Real-Time PCR System; Applied Biosystems) with SYBR Green DNA binding dye. *Gapdh* was chosen as the internal control for each sample.

The following primer sequences were used: for *Dec1*, 5′-AGCAG TGGTT CTGGA GCTTA C-3′ and 5′-TCTTC CCGAC AAATC ACCAG C-3′; for *Dec2*, 5′-CCGAA CATCT GAAAT TGACA ACAC-3′ and 5′-CGGCT TTTCC TGGGC ATTC-3′; for *E4bp4*, 5′-GGTTA CAGCC GCCCT TTCT-3′ and 5′-GTCCG GCACA GGGTA AATCT-3′; for *Gapdh*, 5′-ACGGG AAGCT CACTG GCATG GCCTT-3′ and 5′-CATGA GGTCC ACCAC CCTGT TGCTG-3′.

Hyperosmotic pulse, alkaline, and acid treatments

For the hyperosmotic pulse treatment, sorbitol was added to the cultured media as previously described (25). In brief, the whole cultured media (2.5 mL) were removed, and 0.88 mL of the used media were rapidly returned back to the original wells after mixing with 0.12 mL of 5 M sorbitol in the fresh media (final 600 mM). After 30-min incubation, the hypertonic media were replaced by the residual used media that had been kept at 37°C (see also Fig. 1A).

In control (mock) experiments, the same volume of the media without sorbitol was added. The measured osmolarity was

832 ± 7.1 and 300 ± 3.0 mOsm/kg H_2O for the sorbitol and mock treatments, respectively. For acid or alkaline treatment, a minimal volume of 1 *M* HCl or 1 *M* NaOH solution was added to the cultured media as previously described (30, 67). In control (mock) experiments, the same volume of distilled water was added. The measured pH was 6.6, 7.4, or 7.0 for the acid, alkaline, or mock treatment, respectively.

Calculation of the circadian period, amount of phase shift, and damping rate

For determination of the circadian period, the raw data of bioluminescence rhythms were detrended by subtracting their 24-h moving averages and were smoothed by their 2-h moving averages. The circadian period was calculated from the slope of a regression line fitted to time points of consecutive peaks and troughs of cellular rhythms by the least-squares method. At least 5 time points of peaks and troughs of cellular rhythms were selected for the fitting.

For determination of the phase shift, the regression lines before and after the stimulus were extrapolated to a time point of the stimulus and the phase difference at the time point was calculated, where any time point(s) within 5 h after the stimuli was eliminated. For determination of the damping rate, the amplitude of each circadian cycle was calculated from the difference in bioluminescence between the peak and trough of the detrended and smoothed rhythms. The damping rate was calculated from the exponent of a regression curve fitted to the amplitudes of circadian cycles.

Genome editing with CRISPR-Cas9 systems

For deleting the C-term region of CLOCK protein, targeting sequences were determined by CRISPRdirect (https://crispr.dbcls.jp) (39). pX459 plasmid containing a chimeric guide RNA and SpCas9 expression cassette (Cat. No. 42230; Addgene) (11, 51) was digested by *Bbs*I restriction enzyme, and the targeting sequences were inserted. PER2::LUC MEFs were transfected with the pX459 plasmid by Lipofectamine3000 Reagent (Thermo Fisher Scientific) according to the manufacturer's protocol. After the transfection, cells were seeded at a density of one cell per well in 96-well plates. For isolating cell lines, wells containing a single colony were selected by CloneSelect Imager (Molecular Device). The genome DNA sequences of the target site were read by direct Sanger sequencing.

Antibodies for immunoblot analysis

In immunoblot analysis, antibodies used were anti-AKT antibody (No. 2920; Cell Signaling Technology), anti-phospho-AKT (Ser473) antibody (No. 9271; Cell Signaling Technology), and anti-beta-actin AC-74 antibody (No. A2228; Sigma). The bound primary antibodies were detected by horseradish peroxidase-conjugated antirabbit IgG antibody (Kirkegaard & Perry Laboratories) or antimouse IgG antibody (Kirkegaard & Perry Laboratories).

Immunoprecipitation of CLOCK–BMAL1 complex

HEK293T cells were plated on 10 cm dishes 24 h before the experiments, and Myc-CLOCK/pSG5 (69) and Flag-BMAL1/pcDNA3.1 (69) were transiently transfected by using polyethylenimine. After 24 h, the cultured media were changed to the fresh one supplemented with MK2206 (final 1.0 μM; ChemScene) and incubated for another 16 h. After osmotic stimuli, all media were removed at indicated time points, and the cells were harvested with ice-cold PBS. The samples were centrifuged (4°C, 700 *g*, 1 min), and the supernatant was removed.

Cells were dissolved in 1.8 mL lysis buffer (50 m*M* NH_4HCO_3, 137 m*M* NaCl, 1 m*M* ethylenediaminetetraacetic acid, 5% glycerol, 0.05% Lubrol PX, 1 m*M* dithiothreitol, 1 m*M* phenylmethylsulfonyl fluoride, 4 μg/μL aprotinin, 4 μg/μL leupeptin, 50 m*M* NaF, 1 m*M* Na_3VO_4) and centrifuged (4°C, 21,600 *g*, 10 min). After a brief centrifugation, α-Flag M2 Affinity Gel (Sigma) was added to the supernatant and rotated at 4°C for 2 h.

After a brief centrifugation, the precipitate was washed once with Wash buffer A (50 m*M* NH_4HCO_3, 180 m*M* NaCl, 0.05% Lubrol) and washed twice with Wash buffer B (50 m*M* NH_4HCO_3, 180 m*M* NaCl). Elution buffer (50 m*M* NH_4HCO_3, 137 m*M* NaCl, 150 ng/μl Flag peptide, 12 m*M* sodium deoxycholate) was added to the precipitate, and was agitated at room temperature for 15 min. After a brief centrifugation, the supernatant was collected as an elution fraction containing eluted CLOCK–BMAL1 complex.

Preparation of digested peptides derived from CLOCK–BMAL1 complex

Enzymatic digestion of proteins in the elution fraction was performed according to a phase transfer surfactant (PTS) protocol as previously described (25) with modifications. For detecting CLOCK phosphorylation, the elution samples in 100 μL PTS buffer (100 m*M* NH_4HCO_3, 12 m*M* sodium deoxycholate, 12 m*M* sodium *N*-lauroylsarcosinate) containing phosphatase inhibitor cocktail 2 and 3 (Sigma) were reduced by incubation with 10 m*M* DTT at 60°C for 30 min, and then alkylated by incubation with 22 m*M* iodoacetamide at 37°C for 30 min in the dark. The resultant protein samples were diluted with 100 m*M* NH_4HCO_3 solution up to 500 μL, and digested with 0.4 μg of trypsin (Sigma) by incubation at 37°C for 18 h in the dark.

After the digestion, an equal volume of ethyl acetate was added to the samples, and the mixture was acidified with 0.5% TFA and mixed well to transfer the detergents into the organic phase. After the samples were centrifuged at 15,700 *g* for 1 min at room temperature, the aqueous phase containing peptides was collected. The sample was concentrated by a centrifugal evaporator (EYELA) and desalted using MonoSpin C18 column (GL Sciences). The eluate was dried by the evaporator before LC-MS/MS analysis.

LC-MS/MS-based proteome analysis for detecting CLOCK phosphorylation

The dried and desalted peptides were dissolved in distilled water containing 2% acetonitrile and 0.1% TFA. The LC-MS/MS analyses were performed using a mass spectrometer (Q Exactive Plus; Thermo Fisher Scientific) equipped with a nano ultra high performance liquid chromatography system (Dionex Ultimate 3000; Thermo Fisher Scientific). The peptides were loaded onto the LC-MS/MS system with a trap column (0.3 × 5 mm, L-column, ODS; Chemicals

Evaluation and Research Institute) and a capillary column (0.1 × 150 mm, L-column, ODS; Chemicals Evaluation and Research Institute) at a flow rate of 20 μL/min.

The loaded peptides were separated by a gradient using mobile phases A (1% formic acid in distilled water) and B (1% formic acid in acetonitrile) at a flow rate of 300 nL/min (0% to 30% B in 35 min, 30% to 50% B in 5 min, 50%–95% B in 0.1 min, 95% B for 9.8 min, 95%–0% B in 0.1 min, and 0% B for 5 min). The eluted peptides were electrosprayed (2.0 kV) and introduced into the MS equipment (positive ion mode, data-dependent MS/MS). Each of the most intense precursor ions (up to top 10) was isolated and fragmented by higher collision energy dissociation with the normalized collision energy (27%).

For full MS scans, the scan range was set to 350–1500 m/z at a resolution of 70,000, and AGC target was set to 3e6 with maximum injection time of 60 ms. For MS/MS scans, precursor isolation window was set to 1.6 m/z at a resolution of 17,500, and AGC target was set to 5e5 with maximum injection time of 60 ms. The Orbitrap mass analyzer was operated with the ''lock mass'' option to perform shotgun detection with high accuracy.

The raw spectra were extracted using Proteome Discoverer 2.2 (Thermo Fisher Scientific), and searched against the human SwissProt database (TaxID = 9606 and subtaxonomies, v2017-10-25), mouse CLOCK, and mouse BMAL1 proteins with the following settings: the parameter of the cleavage was set to trypsin, and the missed cleavage was allowed up to 2. The mass tolerances were set to 10 ppm for precursor ion and 0.05 Da for fragment ion. As for protein modifications, we set carbamidomethylation (+57.021 Da) at Cys as static (fixed) modifications for peptide, oxidation (+15.995 Da) at Met, and phosphorylation (+79.966 Da) at Ser and Thr as dynamic (nonfixed) modifications for peptide, and acetylation (+42.011 Da) at amino-terminus as a dynamic modification for protein terminus. The amount of each peptide was semi-quantified using peak area with Precursor Ions Quantifier in Proteome Discoverer 2.2.

LC-MS/MS-based phosphoproteome analysis

Preparation of digested peptides and LC-MS/MS analysis were performed as described above with the following modifications: MEFs treated with 600 m*M* sorbitol, and indicated inhibitors were harvested and lysed with PTS buffer. The reduced and alkylated protein samples (~ 200 μg) were digested with 2.0 μg of trypsin (Sigma). The desalted peptides were dried and applied to a high-select Fe-NTA phosphopeptide enrichment kit (Thermo Fisher Scientific). The peptides were loaded onto the LC-MS/MS system and separated by a gradient (0% B for 5 min, 0%–30% B for 150 min, 30%–50% B for 10 min, 50%–95% B for 0.1 min, 95% B for 9.8 min, 95%–0% B for 0.1 min, and 0% B for 5 min). For data analysis, the mouse SwissProt database (TaxID 10,090 and subtaxonomies, v2017-10-25) was used.

Kinase-Substrate Enrichment Analysis

KSEA was performed as previously described (10) with some modifications. The resources for kinase-substrate relationship dataset used in this analysis were PhosphoSitePlus (ver. 6.5.9.3; https://www.phosphosite.org/homeAction), RegPhos2.0 (http://140.138.144.141/~RegPhos/index.php), and the Universal Protein Resource (Uniprot; https://www.uniprot.org). For quantitative analysis, we used all the phosphorylation sites that were identified in our phosphoproteome analysis on MEFs.

The amount of each substrate peptide was normalized by an average of the amounts of the substrate peptide in mock samples, and the normalized values were represented as log2-fold changes (positive and negative values indicate an increase and decrease in abundance of the phosphorylated peptide, respectively). These values were subjected to a Python package, Kinact (ver. 0.3) (64), to analyze protein kinase activities by using the kinase-substrate relationship dataset. A kinase activity score was defined as the average of the log2-fold changes of substrate peptides.

Electronic laboratory notebook

Electronic laboratory notebooks were not used.

Authors' Contributions

H.Y. designed the research; H.Y., K.I., T.O., Y.O., and S.I. performed research; H.Y., K.I., T.O., Y.O., and S.K. analyzed data; T.T., K.H., I.N., and H.I. supported the project; H.Y. and Y.F. supervised the whole project; H.Y. and K.I. wrote the draft of the article and Y.F. edited it.

Acknowledgments

We thank Mr. Kento Yoshida, Ms. Yasuko Abe, Ms. Yoko Suehiro, and Ms. Keiko Tominaga for their help with experiments.

Author Disclosure Statement

No competing financial interests exist.

Funding Information

This work was partially supported by Grants-in-Aid for Specially Promoted Research (17H06096; to Y.F.), for Scientific Research (B) (19H03175; to H.Y.), for Transformative Research Areas (B) (21H05130; to H.Y.), and for Challenging Research (Pioneering; 21K18231; to H.Y.) from the Ministry of Education, Culture, Sports, Science and Technology (MEXT) of Japan, by the Precursory Research for Innovative Medical Care (PRIME) from Japan Agency for Medical Research and Development (AMED; 17937210; to H.Y.), and by a Japan Society for the Promotion of Science (JSPS) research fellowship for PD (20J00925; to K.I.).

Supplementary Material

Supplementary Figure S1
Supplementary Figure S2
Supplementary Figure S3
Supplementary Figure S4
Supplementary Figure S5
Supplementary Figure S6
Supplementary Figure S7

References

1. Balsalobre A, Brown SA, Marcacci L, Francois T, Kellendonk C, Reichardt HM, Glunter S, and Schibler U. Resetting of circadian time in peripheral tissues by glucocorticoid signaling. *Science* 289: 2344–2347, 2000.
2. Balsalobre A, Damiola F, and Schibler U. A serum shock induces circadian gene expression in mammalian tissue culture cells. *Cell* 93: 929–937, 1998.
3. Bass J and Lazar MA. Circadian time signatures of fitness and disease. *Science* 354: 994–999, 2016.
4. Bass J and Takahashi JS. Circadian integration of metabolism and energetics. *Science* 330: 1349–1354, 2010.
5. Brown SA, Zumbrunn G, Fleury-Olela F, Preitner N, and Schibler U. Rhythms of mammalian body temperature can sustain peripheral circadian clocks. *Curr Biol* 12: 1574–1583, 2002.
6. Buhr ED, Yoo SH, and Takahashi JS. Temperature as a universal resetting cue for mammalian circadian oscillators. *Science* 330: 379–385, 2010.
7. Bunger MK, Wilsbacher LD, Moran SM, Clendenin C, Radcliffe LA, Hogenesch JB, Simon MC, Takahashi JS, and Bradfield CA. Mop3 is an essential component of the master circadian pacemaker in mammals. *Cell* 103: 1009–1017, 2000.
8. Cao R, Lee B, Cho H, Saklayen S, and Obrietan K. Photic regulation of the mTOR signaling pathway in the suprachiasmatic circadian clock. *Mol Cell Neurosci* 38: 312–324, 2008.
9. Cao R, Li A, Cho H, Lee B, and Obrietan K. Mammalian target of rapamycin signaling modulates photic entrainment of the suprachiasmatic circadian clock. *J Neurosci* 30: 6302–6314, 2010.
10. Casado P, Cosulich SC, Guichard S, Vanhaesebroeck B, Joel S, and Cutillas PR. Kinase-substrate enrichment analysis provides insights into the heterogeneity of signaling pathway activation in leukemia cells. *Sci Signal* 6: rs6, 2013.
11. Cong L, Ran FA, Cox D, Lin S, Barretto R, Habib N, Hsu PD, Wu X, Jiang W, Marraffini LA, and Zhang F. Multiplex genome engineering using CRISPR/Cas systems. *Science* 339: 819–824, 2013.
12. Crosby P, Hamnett R, Putker M, Clevers H, Bechtold DA, Neill JSO, Crosby P, Hamnett R, Putker M, Hoyle NP, Reed M, Karam CJ, Maywood ES, Stangherlin A, Chesham JE, Hayter EA, Rosenbrier-ribeiro L, Newham P, Clevers H, Bechtold DA, and Neill JSO. Insulin/IGF-1 drives PERIOD synthesis to entrain circadian rhythms with feeding time. *Cell* 177: 896–909, 2019.
13. Dang F, Sun X, Ma X, Wu R, Zhang D, Chen Y, Xu Q, Wu Y, and Liu Y. Insulin post-transcriptionally modulates Bmal1 protein to affect the hepatic circadian clock. *Nat Commun* 7: 12696–12707, 2016.
14. Doi M, Nakajima Y, Okano T, and Fukada Y. Light-induced phase-delay of the chicken pineal circadian clock is associated with the induction of cE4bp4, a potential transcriptional repressor of cPer2 gene. *Proc Natl Acad Sci U S A* 98: 8089–8094, 2001.
15. Dudek M, Boot-handford RP, Meng Q, Dudek M, Gossan N, Yang N, Im H, Ruckshanthi JPD, Yoshitane H, Li X, Jin D, Wang P, Boudiffa M, Bellantuono I, Fukada Y, Boot-Handford RP, and Meng Q. The chondrocyte clock gene Bmal1 controls cartilage homeostasis and integrity. *J Clin Invest* 126: 365–376, 2016.
16. Dunlap JC. Molecular bases for circadian clocks. *Cell* 96: 271–290, 1999.
17. Edgar RS, Green EW, Zhao Y, van Ooijen G, Olmedo M, Qin X, Xu Y, Pan M, Valekunja UK, Feeney KA, Maywood ES, Hastings MH, Baliga NS, Merrow M, Millar AJ, Johnson CH, Kyriacou CP, O'Neill JS, and Reddy AB. Peroxiredoxins are conserved markers of circadian rhythms. *Nature* 485: 459–464, 2012.
18. Fayard E, Lionel A, Baudry A, and Hemmings BA. Protein kinase B/Akt at a glance. *J Cell Sci* 118: 5675–5678, 2005.
19. Feeney K a, Hansen LL, Putker M, Olivares-Yanez C, Day J, Eades LJ, Larrondo LF, Hoyle NP, O'Neill JS, and van Ooijen G. Daily magnesium fluxes regulate cellular timekeeping and energy balance. *Nature* 532: 375–379, 2016.
20. Gallego M and Virshup DM. Post-translational modifications regulate the ticking of the circadian clock. *Nat Rev Mol Cell Biol* 8: 139–148, 2007.
21. Harada Y, Sakai M, Kurabayashi N, Hirota T, and Fukada Y. Ser-557-phosphorylated mCRY2 is degraded upon synergistic phosphorylation by glycogen synthase kinase-3β. *J Biol Chem* 280: 31714–31721, 2005.
22. Hirota T and Fukada Y. Resetting mechanism of central and peripheral circadian clocks in mammals. *Zoolog Sci* 21: 359–368, 2004.
23. Honma S, Kawamoto T, Takagi Y, Fujimoto K, Sato F, Noshiro M, Kato Y, and Honma K. Dec1 and Dec2 are regulators of the mammalian molecular clock. *Nature* 419: 841–844, 2002.
24. Ichijo H, Nishida E, Irie K, ten Dijke P, Saitoh M, Moriguchi T, Takagi M, Matsumoto K, Miyazono K, and Gotoh Y. Induction of apoptosis by ASK1, a mammalian MAPKKK that activates SAPK/JNK and p38 signaling pathways. *Science* 275: 90–94, 1997.
25. Imamura K, Yoshitane H, Hattori K, Yamaguchi M, Yoshida K, Okubo T, Naguro I, Hidenori I, and Fukada Y. ASK family kinases mediate cellular stress and redox signaling to circadian clock. *Proc Natl Acad Sci U S A* 114: 3646–3651, 2018.
26. Iriyama T, Takeda K, Nakamura H, Morimoto Y, Kuroiwa T, Mizukami J, Umeda T, Noguchi T, Naguro I, Nishitoh H, Saegusa K, Tobiume K, Homma T, Shimada Y, Tsuda H, Aiko S, Imoto I, Inazawa J, Chida K, Kamei Y, Kozuma S, Taketani Y, Matsuzawa A, and Ichijo H. ASK1 and ASK2 differentially regulate the counteracting roles of apoptosis and inflammation in tumorigenesis. *EMBO J* 28: 843–853, 2009.
27. Jacinto E, Facchinetti V, Liu D, Soto N, Wei S, Jung SY, Huang Q, Qin J, and Su B, SIN1/MIP1 maintains rictor-mTOR complex integrity and regulates Akt phosphorylation and substrate specificity. *Cell* 127: 125–137, 2006.
28. Kamizono S, Duncan GS, Seidel MG, Morimoto A, Hamada K, Grosveld G, Akashi K, Lind EF, Haight JP, Ohashi PS, Look AT, and Mak TW. Nfil3/E4bp4 is required for the development and maturation of NK cells in vivo. *J Exp Med* 206: 2977–2986, 2009.
29. Kawarazaki Y, Ichijo H, and Naguro I. Apoptosis signal-regulating kinase 1 as a therapeutic target. *Expert Opin Ther Targets* 18: 651–664, 2014.
30. Kon N, Hirota T, Kawamoto T, Kato Y, Tsubota T, and Fukada Y. Activation of TGF-beta/activin signalling resets the circadian clock through rapid induction of Dec1 transcripts. *Nat Cell Biol* 10: 1463–1469, 2008.
31. Kondratov RV, Kondratova AA, Gorbacheva VY, Vykhovanets OV, and Antoch MP. Early aging and age-related

pathologies in mice deficient in BMAL1, the core component of the circadian clock. *Genes Dev* 20: 1868–1873, 2006.
32. Lee C, Etchegaray JP, Cagampang FR, Loudon SI, and Reppert SM. Posttranslational mechanisms regulate the mammalian circadian clock. *Cell* 107: 855–867, 2001.
33. Lipton JO, Yuan ED, Asara JM, Sahin M, Lipton JO, Yuan ED, Boyle LM, Ebrahimi-Fakhari D, Kwiatkowski E, Nathan A, Davis F, Asara JM, and Sahin M. The circadian protein BMAL1 regulates translation in response to S6K1-mediated phosphorylation. *Cell* 161: 1138–1151, 2015.
34. Liu R, Liu D, and Xing M. The Akt inhibitor MK2206 synergizes, but perifosine antagonizes, the $BRAF^{V600E}$ inhibitor PLX4032 and the MEK1/2 inhibitor AZD6244 in the inhibition of thyroid cancer cells. *J Clin Endocrinol Metab* 97: E173–E182, 2012.
35. Luciano AK, Zhou W, Santana JM, Kyriakides C, Velazquez H, and Sessa WC. CLOCK phosphorylation by AKT regulates its nuclear accumulation and circadian gene expression in peripheral tissues. *J Biol Chem* 293: 9126–9136, 2018.
36. Ma D, Panda S, and Lin JD. Temporal orchestration of circadian autophagy rhythm by C/EBPβ. *EMBO J* 30: 4642–4651, 2011.
37. Matsuzawa A, Saegusa K, Noguchi T, Sadamitsu C, Nishitoh H, Nagai S, Koyasu S, Matsumoto K, Takeda K, and Ichijo H. ROS-dependent activation of the TRAF6-ASK1-p38 pathway is selectively required for TLR4-mediated innate immunity. *Nat Immunol* 6: 587–592, 2005.
38. Naguro I, Umeda T, Kobayashi Y, Maruyama J, Hattori K, Shimizu Y, Kataoka K, Kim-Mitsuyama S, Uchida S, Vandewalle A, Noguchi T, Nishitoh H, Matsuzawa A, Takeda K, and Ichijo H. ASK3 responds to osmotic stress and regulates blood pressure by suppressing WNK1-SPAK/OSR1 signaling in the kidney. *Nat Commun* 3: 1285–1295, 2012.
39. Naito Y, Hino K, Bono H, and Ui-Tei K. Genome analysis CRISPRdirect: software for designing CRISPR/Cas guide RNA with reduced off-target sites. *Bioinformatics* 31: 1120–1123, 2015.
40. Nakahata Y, Sahar S, Astarita G, Kaluzova M, and Sassone-Corsi P. Circadian control of the NAD^+ salvage pathway by CLOCK-SIRT1. *Science* 324: 654–657, 2009.
41. Nakashima A, Kawamoto T, Honda KK, Ueshima T, Noshiro M, Iwata T, Fujimoto K, Kubo H, Honma S, Yorioka N, Kohno N, and Kato Y. DEC1 modulates the circadian phase of clock gene expression. *Mol Cell Biol* 28: 4080–4092, 2008.
42. Nicholson KM and Anderson NG. The protein kinase B/Akt signalling pathway in human malignancy. *Cell Signal* 14: 381–395, 2002.
43. Noguchi T, Takeda K, Matsuzawa A, Saegusa K, Nakano H, Gohda J, Inoue JI, and Ichijo H. Recruitment of tumor necrosis factor receptor-associated factor family proteins to apoptosis signal-regulating kinase 1 signalosome is essential for oxidative stress-induced cell death. *J Biol Chem* 280: 37033–37040, 2005.
44. O'Neill JS and Reddy AB. Circadian clocks in human red blood cells. *Nature* 469: 498–503, 2011.
45. Pal SK, Reckamp K, Yu H, and Figlin RA. Akt inhibitors in clinical development for the treatment of cancer. *Expert Opin Investig Drugs* 19: 1355–1366, 2010.
46. Papp SJ, Huber A-L, Jordan SD, Kriebs A, Nguyen M, Moresco JJ, Yates JR, III, and Lamia KA. DNA damage shifts circadian clock time via Hausp-dependent Cry1 stabilization. *Elife* 4: e4883–e5001, 2015.
47. Peek CB, Affinati AH, Ramsey KM, Kuo H-Y, Yu W, Sena LA, Ilkayeva O, Marcheva B, Kobayashi Y, Omura C, Levine DC, Bacsik DJ, Gius D, Newgard CB, Goetzman E, Chandel NS, Denu JM, Mrksich M, and Bass J. Circadian clock NAD^+ cycle drives mitochondrial oxidative metabolism in mice. *Science* 342: 591–599, 2013.
48. Plescher M, Teleman AA, and Demetriades C. TSC2 mediates hyperosmotic stress-induced inactivation of mTORC1. *Sci Rep* 5: 13828, 2015.
49. Ramanathan C, Kathale ND, Liu D, Lee C, Freeman A, Hogenesch JB, Cao R, and Liu AC. mTOR signaling regulates central and peripheral circadian clock function. *PLoS Genet* 14: e1007369, 2018.
50. Ramsey KM, Yoshino J, Brace CS, Abrassart D, Kobayashi Y, Marcheva B, Hong H-K, Chong JL, Buhr ED, Lee C, Takahashi JS, Imai S-I, and Bass J. Circadian clock feedback cycle through NAMPT-mediated NAD^+ biosynthesis. *Science* 324: 651–654, 2009.
51. Ran FA, Hsu PD, Wright J, Agarwala V, Scott DA, and Zhang F. Genome engineering using the CRISPR-Cas9 system. *Nat Protoc* 8: 2281–2308, 2013.
52. Rossner MJ, Oster H, Wichert SP, Reinecke L, Wehr MC, Eichele G, Taneja R, and Nave K. Disturbed clockwork resetting in Sharp-1 and Sharp-2 single and double mutant mice. *PLoS One* 3: e2762–e2773, 2008.
53. Saitoh M, Nishitoh H, Fujii M, Takeda K, Tobiume K, Sawada Y, Kawabata M, Miyazono K, and Ichijo H. Mammalian thioredoxin is a direct inhibitor of apoptosis signal-regulating kinase (ASK) 1. *EMBO J* 17: 2596–2606, 1998.
54. Sarbassov DD, Ali SM, and Sabatini DM. Growing roles for the mTOR pathway. *Curr Opin Cell Biol* 17: 596–603, 2005.
55. Sarbassov DD, Guertin DA, Ali SM, and Sabatini DM. Phosphorylation and regulation of Akt/PKB by the rictor-mTOR complex. *Science* 307: 1098–1102, 2005.
56. Sato F, Muragaki Y, Kawamoto T, Fujimoto K, Kato Y, and Zhang Y. Rhythmic expression of DEC2 protein in vitro and in vivo. *Biomed Rep* 4: 704–710, 2016.
57. Schibler U and Sassone-Corsi P. A web of circadian pacemakers. *Cell* 111: 919–922, 2002.
58. Sutherland C, Leighton IA, and Cohen P. Inactivation of glycogen synthase kinase-3β by phosphorylation: new kinase connections in insulin and growth-factor signalling. *Biochem J* 296: 15–19, 1993.
59. Takeda K, Komuro Y, Hayakawa T, Oguchi H, Ishida Y, Murakami S, Noguchi T, Kinoshita H, Sekine Y, Iemura S, Natsume T, and Ichijo H. Mitochondrial phosphoglycerate mutase 5 uses alternate catalytic activity as a protein serine/threonine phosphatase to activate ASK1. *Proc Natl Acad Sci U S A* 106: 12301–12305, 2009.
60. Takeda K, Noguchi T, Naguro I, and Ichijo H. Apoptosis signal-regulating kinase 1 in stress and immune response. *Annu Rev Pharmacol Toxicol* 48: 199–225, 2008.
61. Tamai S, Imaizumi K, Kurabayashi N, Nguyen MD, Abe T, Inoue M, Fukada Y, and Sanada K. Neuroprotective role of the basic leucine zipper transcription factor NFIL3 in models of amyotrophic lateral. *J Biol Chem* 289: 1629–1638, 2014.

62. Watanabe K, Morishita K, Zhou X, Shiizaki S, Uchiyama Y, Koike M, Naguro I, and Ichijo H. Cells recognize osmotic stress through liquid–liquid phase separation lubricated with poly(ADP-ribose). *Nat Commun* 12: 1353–1367, 2021.
63. Watanabe K, Umeda T, Niwa K, Naguro I, and Ichijo H. A PP6-ASK3 module coordinates the bidirectional cell volume regulation under osmotic stress. *Cell Rep* 22: 2809–2817, 2018.
64. Wirbel J, Cutillas P, and Saez-rodriguez J. Phosphoproteomics-based profiling of kinase activities in cancer cells. *Methods Mol Biol* 1711: 103–132, 2018.
65. Yagita K, Tamanini F, van Der Horst GT, and Okamura H. Molecular mechanisms of the biological clock in cultured fibroblasts. *Science* 292: 278–281, 2001.
66. Yoo SH, Yamazaki S, Lowrey PL, Shimomura K, Ko CH, Buhr ED, Siepka SM, Hong H-K, Oh WJ, Menaker M, and Takahashi JS. PERIOD2::LUCIFERASE real-time reporting of circadian dynamics reveals persistent circadian oscillations in mouse peripheral tissues. *Proc Natl Acad Sci U S A* 101: 5339–5346, 2004.
67. Yoshitane H, Asano Y, Sagami A, Sakai S, Suzuki Y, Okamura H, Iwasaki W, Ozaki H, and Fukada Y. Functional D-box sequences reset the circadian clock and drive mRNA rhythms. *Commun Biol* 2: 300–309, 2019.
68. Yoshitane H, Honma S, Imamura K, Nakajima H, Nishide S, Ono D, Kiyota H, Shinozaki N, Matsuki H, Wada N, Doi H, Hamada T, Honma K, and Fukada Y. JNK regulates the photic response of the mammalian circadian clock. *EMBO Rep* 13: 455–461, 2012.
69. Yoshitane H, Takao T, Satomi Y, Du NH, Okano T, and Fukada Y. Roles of CLOCK phosphorylation in suppression of E-box-dependent transcription. *Mol Cell Biol* 29: 3675–3686, 2009.
70. Zheng X and Sehgal A. AKT and TOR signaling set the pace of the circadian pacemaker. *Curr Biol* 20: 1203–1208, 2010.

Address correspondence to:
Dr. Yoshitaka Fukada
Department of Biological Sciences
School of Science
The University of Tokyo
Hongo 7-3-1
Bunkyo-ku
Tokyo 113-0033
Japan

E-mail: sfukada@mail.ecc.u-tokyo.ac.jp

Dr. Hikari Yoshitane
Circadiain Clock Project
Tokyo Metropolitan Institute of Medical Science
Kamikitazawa 2-1-6
Setagaya-ku
Tokyo 156-8506
Japan

E-mail: yoshitane-hk@igakuken.or.jp

Date of first submission to ARS Central, April 8, 2021; date of final revised submission, December 27, 2021; date of acceptance, December 31, 2021.

Abbreviations Used

ASK = apoptosis signal-regulating kinase
BMAL1 = brain and muscle Arnt-like protein-1
C-terminal = carboxyl-terminal
CLOCK = circadian locomotor output cycles caput
Dec = deleted in esophageal cancer
DMSO = dimethyl sulfoxide
E4bp4 = E4 promoter-binding protein 4 (also known as NFIL 3)
GSK = glycogen synthase kinase
HEK = human embryonic kidney
KSEA = Kinase-Substrate Enrichment Analysis
LC-MS/MS = liquid chromatography mass/mass spectrometry
LUC = luciferase
MAPK = mitogen-activated protein kinase
MEF = mouse embryonic fibroblast
mRNA = messenger RNA
mTOR = mechanistic target of rapamycin
NAD^+ = nicotinamide adenine dinucleotide
N.D. = not detected
OSR = oxidative stress-responsive kinase
PAM = protospacer adjacent motif
PBS = phosphate buffered saline
PCR = polymerase chain reaction
PTS = phase transfer surfactant
RVI = regulatory volume increase
SCN = suprachiasmatic nuclei
SEM = standard error of the mean
sgRNA = single guide RNA
SPAK = STE20/SPS1-related proline/alanine-rich kinase
TKO = triple knockout
WNK = with no lysine (K) protein kinase
WT = wild type